

AD-A114 525

WASHINGTON UNIV SEATTLE DEPT OF MECHANICAL ENGINEERING

F/8 20/11

DYNAMIC CRACK BRANCHING - A PHOTOELASTIC EVALUATION (U)

MAY 82 M RAMULU, A S KOBAYASHI, B S KANG

N00014-76-C-0060

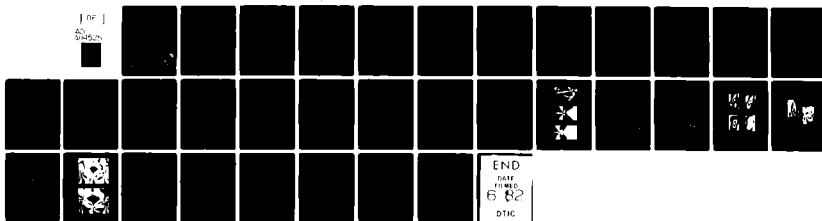
UNCLASSIFIED

UWA/DME/TR-82/43

NL

1 of 1

50-108



END

DATE

FORMED

6 82

DTIC

AD A114525

DTIC FILE COPY

Office of Naval Research  
Contract N00014-76-C-0060 NR 064-478  
Technical Report No. UWA/DME/TR-82/43

DYNAMIC CRACK BRANCHING - A PHOTOELASTIC EVALUATION

by

M. Ramulu, A. S. Kobayashi and B.S.-J. Kang

May 1982

The research reported in this technical report was made possible through support extended to the Department of Mechanical Engineering, University of Washington, by the Office of Naval Research under Contract N00014-76-C-0060 NR 064-478. Reproduction in whole or in part is permitted for any purpose of the United States Government.

Department of Mechanical Engineering  
College of Engineering  
University of Washington

DTIC  
ELECTE  
MAY 18 1982  
H

DISTRIBUTION STATEMENT A  
Approved for public release;  
Distribution Unlimited

# Dynamic Crack Branching - A Photoelastic Evaluation

by

M. Ramulu, A. S. Kobayashi and B. S.-J. Kang

Department of Mechanical Engineering  
College of Engineering  
University of Washington  
Seattle, WA 98195

## ABSTRACT

A necessary and sufficient condition for crack branching based on a crack branching stress intensity factor,  $K_{Ib}$ , accompanied by a minimum characteristic distance of  $r_c$  is proposed. This crack branching criterion is evaluated by dynamic photoelastic experiments involving crack branching of six single-edged notch specimens and six wedge-loaded rectangular double cantilever beam specimens. Consistent crack branching at  $K_{Ib} = 2.04 \text{ MPa}\sqrt{\text{m}}$  and  $r_c = 1.3 \text{ mm}$  verified this crack branching criterion. The crack branching angle predicted by this crack branching criterion agreed well with those measured in the crack branching experiments.

Accession For	
NTIS GRA&I	<input checked="checked" type="checkbox"/>
DTIC TAB	<input type="checkbox"/>
Unannounced	<input type="checkbox"/>
Justification	
By	
Distribution/	
Availability Codes	
Dist	Avail and/or Special
A	



## INTRODUCTION

Literature on crack branching criteria can be grouped into two categories of dynamic crack tip stress field distortion [1,2,3]\* and initiation of the secondary cracks [4-7]. While the former relates only to the singular stress field at the crack tip, the latter incorporates the nonsingular stress components. Studies on the crack tip stress field can also be divided into pre- and post-branching analyses. Pre-branching analysis normally leads to a branching criterion, while direction of the branched crack and its propagation are studied in post-branching analysis. An excellent review of such crack branching analysis can be found in Reference [7].

Crack branching has been frequently observed during the ten plus years of dynamic fracture research at the University of Washington [8] and at the University of Maryland [9]. Earlier attempts to evaluate these crack branching results were hampered by the lack of adequate data reduction procedure as well as by the paucity of theoretical understanding on elastodynamic crack propagation. Much of these obstacles have removed today and thus, it appears apropos to re-evaluate these photoelastic data on crack branching in view of the available new data reduction procedure [10]. This data analysis will be preceded by a brief review of existing crack branching criteria, after which a new crack branching criterion will be presented.

---

\*Numbers in bracket refer to references at the end of this paper.

## BRIEF REVIEW OF CRACK BRANCHING CRITERIA

The most popularly held cause of dynamic crack branching is the pre-branching distortion of the crack tip stress field at a critical crack velocity. Yoffe's theoretical analysis [1] of a constant velocity crack showed that at a crack velocity of about  $c/c_1 = 0.33^*$ , the maximum circumferential stress,  $\sigma_{\theta\theta}^{**}$ , shifted away from its original location of  $\theta = 0$  at a lower crack velocity. This crack branching criterion based on dynamic crack kinking was followed by that of Craggs [11], who derived a critical crack velocity of  $c/c_1 = 0.40$  for a propagating semi-infinite crack. Unfortunately, experimentally measured crack velocities never attained the high velocity predicted by this critical crack velocity criterion. Although Döll measured a branching crack velocity of  $c/c_1 \approx 0.28$  and  $0.3$  in glass, [12], but the crack branching velocities in steels reported by Irwin [6], Hahn et al. [13], Congleton et al. [5], and in photoelastic polymers reported by A. S. Kobayashi et al. [8], and by T. Kobayashi and Dally [14] were less than  $c/c_1 = 0.25$ . Also, the precise ultrasonic ripple marking techniques used to mark instantaneous crack front by Kerkhoff [15] showed only a ten percent decrease in crack speed in glass immediately after branching, while Schardin [16] observed no change in crack velocity in plate glass. Acloque [17] observed only a six percent decrease in crack velocities immediately after branching in prestressed glass. Thus, the experimentally observed lower branching velocities, which hardly decreased after crack branching, showed that the postulated critical crack velocity could not be a prerequisite to crack branching in these materials.

-----  
\* $c$  and  $c_1$  are crack velocity and dilatational stress wave velocity, respectively.

\*\*In terms of polar coordinate  $(r, \theta)$  with origin at the crack tip.

Since crack branching is also observed at extremely low crack velocity, such as that in stress corrosion cracking, other crack tip parameters such as the stress intensity factor, which could trigger branching of a crack propagating at any crack velocity must be sought. For example, attempts have been made to determine experimentally a critical crack branching stress intensity factor,  $K_{Ib}$ . Kobayashi et al. [8] showed that crack branching occurred in Homalite-100 single edge notch (SEN) specimens when  $K_I$  reached a maximum value of 3.6 times its fracture toughness,  $K_{IC}$ . Dally et al. [9,14] obtained a  $K_{Ib} = 3.8 K_{IC}$  from SEN, double cantilever beam (DCB) and compact specimens when the cracks are propagating at terminal velocity in Homalite100.

A crack kinking criterion, which is based on the development of secondary cracks in a region off-axis to the primary crack, is also an attractive alternate since the crack kinking angle is governed by the dynamic crack tip state of stress. Historically, Clark and Irwin [18] concluded that branching occurs by advanced off-axis cracking under critical stress intensity factor,  $K_{Ib}$  at a limiting crack velocity which was smaller than those of Yoffe and Craggs. These advanced cracks created crack surface of increasing roughness which were associated with increasing stress and velocity and which usually terminated after crack branching.

#### CRACK BRANCHING ANGLE

A characteristic feature of a branched crack is the crack branching angle and many attempts have been made to predict this crack branching. Sih [19] used the pre-branching minimum strain energy density to predict a branching angle of 15-18 degrees which varies with Poisson's ratio. Kitagawa [20] and Kalthoff [21] used the static post branching state of stress

of a symmetrically branched edged cracks and postulated that the small initial wedge angle between two branched crack was governed by a vanishing mode II stress intensity factor, i.e.,  $K_{II} = 0$ . Kitagawa et al. predicted a branching angle of 30-40 degrees while Kalthoff's predicted branching angle of 28 degrees agreed with his measured angle in fracturing glass.

The branching angles measured by Christie [22] in an SEN specimen impacted by stress waves was about 25 degrees, while Congleton [5] observed branching angles of about 30-40 degrees in center and edge-notched steel plates and 70-80 degrees in bursting steel tubes. It will be shown later that this variation in measured crack branching angles can be attributed to the influence of a non-singular stress terms which govern the direction of crack branching in various fracture specimen geometry.

#### CRACK BRANCHING CRITERION

As described above, experimental evidences indicate that dynamic crack branching at a terminal crack velocity is accompanied by a critical dynamic stress intensity factor and that the crack branching angles associated with each specimen configuration are very similar. A plausible crack branching criterion would be to postulate that the crack branching stress intensity factor,  $K_{Ib}$ , as a necessary condition accompanied by a sufficient condition for crack kinking which governs the crack branching angle. The former necessary condition is supported by the crack branching data which shows that  $K_{Ib}$  is about four times its fracture toughness in Homalite-100.

As for the latter sufficient condition, either of the two dynamic crack curving criteria [23] advanced by the authors can be used to estimate the crack branching angle. These dynamic crack kinking criteria are derived from the near field, mixed mode elasto-dynamic state of stress

associated with a crack tip propagating at constant velocity. The dynamic state of crack tip stress field is given by Freund [24] in terms of local rectangular and polar coordinates of  $(x,y)$  and  $(r,\theta)$ , respectively, and the mode I and II dynamic stress intensity factors,  $K_I$  and  $K_{II}^*$ , respectively. The second order term of  $\sigma_{ox}$ , which is acting parallel to the direction of crack extension, is also included in the above crack tip state of stress so that crack kinking can be triggered at crack velocities lower than those of Yoffe [1] and Craggs [11]. The two crack kinking criteria based on this dynamic crack tip stress are the maximum circumferential stress and the minimum strain energy density criteria, both of which will predict nearly identical crack kinking angles in the crack velocity range of  $c/c_1 < 0.2$ . Thus for brevity, only the crack kinking criterion based on the maximum circumferential stress criterion will be discussed in this paper.

The angle,  $\theta_c$ , at which circumferential stress,  $\sigma_{\theta\theta}$ , is maximum, when evaluated in conjunction with a pure mode I dynamic crack tip state of stress will yield a transcendental relation between the critical values of  $\theta$  and  $r$  as

$$\begin{aligned}
 r = \frac{1}{4\pi} \left[ \left( \frac{K_I}{\sigma_{ox}} \right) \frac{B_1(c)}{\sin 2\theta} \{ ((S_1^2 - S_2^2) - (1 + S_1^2) \cos 2\theta) \frac{\partial f_{11}}{\partial \theta} \right. \\
 + 2(1 + S_1^2) \sin 2\theta f_{11} + \frac{4S_1 S_2}{1 + S_2^2} \cos 2\theta \frac{\partial f_{22}}{\partial \theta} \\
 - 2 \frac{4S_1 S_2}{1 + S_2^2} \sin 2\theta f_{22} - (2S_1 \sin 2\theta) \left( \frac{\partial g_{11}}{\partial \theta} - \frac{\partial g_{22}}{\partial \theta} \right) \\
 \left. - (4S_1 \cos 2\theta) (g_{11} - g_{22}) \right]^2 \quad (1a)
 \end{aligned}$$

\*The superscript "dyn" to identify dynamic stress intensity factor will not be used in this paper, since all quantities refer to dynamic values.

where

$$\left. \begin{aligned} f_{11} &= [f(c_1) + g(c_1)]^{1/2} \\ g_{11} &= [f(c_1) - g(c_1)]^{1/2} \\ f_{22} &= [f(c_2) + g(c_2)]^{1/2} \\ g_{22} &= [f(c_2) - g(c_2)]^{1/2} \end{aligned} \right\} \quad (1b)$$

$$f(c_1) = \frac{1}{(1 - \frac{c^2}{c_1^2} \sin^2 \theta)^{1/2}} ; \quad g(c_1) = \frac{\cos \theta}{(1 - \frac{c^2}{c_1^2} \sin^2 \theta)^{1/2}} \quad (1c)$$

$$f(c_2) = \frac{1}{(1 - \frac{c^2}{c_2^2} \sin^2 \theta)^{1/2}} ; \quad g(c_2) = \frac{\cos \theta}{(1 - \frac{c^2}{c_2^2} \sin^2 \theta)^{1/2}}$$

$$B_1(c) = \frac{1+s_2^2}{4s_1s_2 - (1+s_2^2)^2} \quad (1d)$$

$$s_1^2 = 1 - \frac{c^2}{c_1^2} ; \quad s_2^2 = 1 - \frac{c^2}{c_2^2} \quad (1e)$$

The critical radial distance was postulated to be a unique material property which was found to be  $r_c = 1.3$  mm for Homalite-100 in Reference [23]. Furthermore, by setting  $\theta = 0$  we obtain a characteristic distance of

$$r_o = \frac{1}{128\pi} \left[ \frac{K_I}{\sigma_{ox}} V_o(c, c_1, c_2) \right]^2 \quad (2a)$$

where

$$\begin{aligned} V_o(c, c_1, c_2) &= B_1(c) \{ -(1+s_2^2)(2-3s_1^2) \\ &\quad - \frac{4s_1s_2}{1+s_2^2} (14+3s_2^2) - 16s_1(s_1-s_2) + 16(1+s_1^2) \} \end{aligned} \quad (2b)$$

and the curving angle  $\theta_c$ , for a stationary crack from Equation (1a) reduces to

$$\theta_c = \cos^{-1} \left[ \frac{1 \pm \sqrt{1 + \frac{1024\pi}{9} r_0 \left( \frac{\sigma_{ox}}{K_I} \right)^2}}{\frac{512\pi}{9} r_0 \left( \frac{\sigma_{ox}}{K_I} \right)} \right] \quad (3)$$

and  $c$ ,  $c_1$  and  $c_2$  are the crack velocity, dilatational and distortional wave velocities, respectively. It can be easily shown that for zero crack velocity or  $c = 0$ , Equation (2) reduces to Streit and Finnie's [25] characteristic radial distance of  $r_0 = \frac{9}{128\pi} \left[ \frac{K_I}{\sigma_{ox}} \right]^2$  for crack kinking of an initially stationary crack. This crack kinking criterion can also be used to estimate the crack branching angle for quasi-static crack branching under stress corrosion cracking conditions, provided a static counterpart of the necessary crack branching stress intensity factor can be established. The dynamic characteristic distance  $r_0$  is always less than the corresponding static  $r_0$  for crack velocities of  $0 < c/c_1 \leq 0.33$  and is insensitive to the sign of  $\sigma_{ox}$ .

The crack kinking criterion thus states that the crack will kink at an angle of  $\theta_c$  when a  $r_0$  associated with the propagating crack tip reaches a critical material property of  $r_c$ . When applied to crack branching, this crack kinking angle is one half of the included crack branching angle since the high crack branching stress intensity will result in sufficient energy release rate to create two kinked cracks simultaneously.

To recapitulate, then, crack branching will occur when the dynamic stress intensity factor reaches  $K_{Ib}$  and the crack will branch at an angle of  $\theta_c$ . In the following, this crack branching criterion will be tested by re-evaluating previous dynamic experiments in which crack branching was observed. Results of eleven dynamic photoelastic results involving SEN and wedge-loaded rectangular DCB (WL-RDCB) fracture specimens are reported in the following.

#### CRACK BRANCHING IN HOMALITE-100 FRACTURE SPECIMENS

##### 1. Homalite-100 SEN Specimens

The SEN specimens considered are of 3.2 mm and 9.5 mm thick Homalite-100 plates with 254 x 254 mm test section loaded in fixed grip configuration. The prescribed boundary conditions included both uniform and linearly decreasing displacements along the fixed gripped edges of the specimen. At fracture load, the crack propagated from the SEN starter crack which was saw cut and chiseled. Further details of the test setup and the test conditions can be found in Reference [26]. Figure 1 shows three frames out of a 16-frame dynamic photoelastic record of a crack propagating and branching in a 3.2 mm thick, 254 x 254 mm Homalite-100 plate loaded under fixed grip linearly varying tension.

Figure 2 shows the dynamic  $K_I$  and  $K_{II}$  variations obtained from the dynamic photoelastic patterns preceding and after crack branching of Figure 1. By extrapolating the dynamic  $K_I$  associated with two branch cracks, an after-branching dynamic stress intensity factor,  $K_I = 1.2 \text{ MPa}\sqrt{\text{m}}$  and  $K_{II} = 0.45 \text{ MPa}\sqrt{\text{m}}$  are obtained. The branching stress intensity factor, i.e. immediately prior to branching is estimated to be  $K_{Ib} = 2.03 \text{ MPa}\sqrt{\text{m}}$ . Also

shown in Figure 2 are the variations in the  $r_0$  values as computed from Equation (2). Note that  $r_0$  reached a minimum value of  $r_c = 1.2$  mm at crack branching.

Figure 3 shows another set of  $K_I$ ,  $K_{II}$  and  $r_0$  for two branch cracks in a similar dynamic photoelastic experiment. By extrapolating the  $K_I$  associated with the two branch cracks, an after-branching  $K_I = 1.2 \text{ MPa}\sqrt{\text{m}}$  and  $K_{II} = -0.1 \text{ MPa}\sqrt{\text{m}}$  are obtained. Immediately prior to branching, the instantaneous dynamic stress intensity factor reached its maximum value of  $2.0 \text{ MPa}\sqrt{\text{m}}$  and is consistent with the previous results. The estimated minimum  $r_0$  at crack branching was  $r_c = 1.3$  mm. Evaluations of four other SEN tests yielded the branching stress intensity factors of  $K_I = 2.00$  and  $2.09 \text{ MPa}\sqrt{\text{m}}$ , as shown in Table 1. The  $r_c$  values ranged from 1.2 to 1.4 mm.

The crack velocities in the above six tests were essentially constant at about  $15 \pm 5$  percent of the dilatational wave velocity,  $c_1 = 2400$  mps. Nevertheless, the crack velocity prior to and after crack branching was very close to the maximum velocity observed in all dynamic fracture tests involving Homalite-100. This so-called terminal velocity varied from test to test in a range of  $0.15$  to  $0.20 c_1$  where the crack always accelerated slightly just prior to crack branching.

The variations in the characteristic distance,  $r_0$ , which was computed from the Equation (2), for the branching cracks in the six tests all reached a minimum value prior to and at crack branching. This minimum value, which was obtained by interpolation at crack branching, was an average of 1.3 mm and is consistent with the previously measured  $r_c$  values for crack curving [23], and is further evidence that  $r_c$  is a material property. Since minimum  $r_0$  or  $r_c$  is derived through  $\sigma_{ox}$ , this  $r_c$  value indicates that  $\sigma_{ox}$  has a significant effect on crack branching.

Table 1 also shows the measured and calculated crack branching angles in the six tests. The crack branching angles, which were computed by Equation (1), for a known  $r_c$ ,  $K_I$  and  $\sigma_{ox}$  are within 10 percent of the measured values, thus validating the use of this crack kinking criterion.

As an interesting sideline, Figure 4 shows the enlarged view of Test No. 85 where an isochromatic pattern of a pure mode II crack tip deformation, i.e. nearly pure shear state of stress, is generated around branched cracks. The mode II stress intensity factor  $K_{II}$  and remote stress  $\sigma_{ox}$  associated with these isochromatics are listed in Table 2. Figure 5 shows that within the 49 micro-second interval, the propagating crack turned about 81 degrees and arrested. The mixed mode stress intensity factors prior to this severe crack kinking were  $K_I = 0$ ,  $K_{II} = 0.41 \text{ MPa}\sqrt{\text{m}}$  and  $\sigma_{ox} = 0.18 \text{ MPa}$ , and predicted a theoretical kinking angle of  $84^\circ$  which agreed well with experimentally measured angle. After crack kinking, the crack arrested and  $K_I = 0.34 \text{ MPa}\sqrt{\text{m}}$ ,  $K_{II} = 0.08 \text{ MPa}\sqrt{\text{m}}$  and  $\sigma_{ox} = 1.4 \text{ MPa}$ . These results show that the crack kinking can also occur under the high  $K_{II}$  state of stress.

## 2. Homalite-100 WL-RDCB Specimen

As mentioned previously, the proposed crack branching criterion should be applicable to quasi-static crack branching where inertia effects in the pre-branched crack are negligible or nonexistent. Experimental data of the former were found in Homalite-100 WL-RDCB specimens where the crack immediately branched after initiating at a blunt starter crack tip. The necessary condition for branching is satisfied by the high  $K_{IQ}^*$  due to the blunt

\*  $K_{IQ}$  is the crack initiation stress intensity factor which is larger than the fracture toughness,  $K_{IC}$ .

crack tip. The crack branching angle, as shown by Equation (3) is a function of  $\sigma_{ox}/K_{IQ}$  and is thus a function of the specimen geometry.

The WL-RDCB fractured specimens considered is 76 x 152 x 9.5 mm thick of the geometry shown in Figure 6. The crack immediately branched and propagated from a single, edge-notched starter crack of length of 24.3 mm to 29.30 mm with a crack tip blunted by drilled hole of diameter of 2.2 mm to 5.0 mm. The branched crack paths of six fractured specimens are also shown in Figure 6.

In all six tests of the WL-RDCB specimens, the crack branched at initiation forming two or three branches. Table 3 summarizes the experimental test specimen information along with the measured branching angle in six WL-RDCB specimens. The angles of deviation of the post branched cracks were measured along the crack path by averaging the measured crack curving angle on front and back surfaces of the fractured specimen. Included angles for all major branches averaged 53.4 degrees, and is twice the branching angle in a SEN specimen. This averaged branch angle agrees with the experimental results of Nakasa and Takei [26] where bending of the SEN specimens due to cantilever loading resulted in a positive  $\sigma_{ox}$  which in turn caused larger branching angles.

Although reliable data on the crack initiation condition was lacking for this series of experiments, the crack branching angle can be estimated from standard finite element analysis. Equation (3) shows  $\theta_c$  involves only the ratio of  $\sigma_{ox}/K_{IQ}$  and the predetermined  $r_c$ , and thus the exact applied loading condition need not be known for estimating the branch angle of an initially stationary crack. In other words, the crack branching angle in this WL-RDCB specimen is governed by the specimen geometry only provided sufficient driving force is provided to branch the crack upon initiation.

However, for a running crack, the dynamic crack branching angle,  $\theta_c$ , involves not only  $\sigma_{ox}/K_I$ ,  $r_o$  but also the crack velocity as given in Equation (1). With a unit vertical wedge loading displacement applied to the specimen,  $K_I$  and  $\sigma_{ox}$  were calculated by least square fitting the following plane stress crack tip displacement field of three to four sets of nodal displacements on the crack surface.

$$u_x = \frac{\sigma_{ox}}{2G} r \left( \frac{1}{1+\nu} \right) \quad (4a)$$

$$u_y = \frac{1}{G} \frac{K_I}{\sqrt{2\pi}} \sqrt{r} \left( \frac{2}{1+\nu} \right) \quad (4b)$$

$G$  and  $\nu$  in Equation (4) are shear modulus and Poisson's ratio, respectively. An average  $K_{IQ}/\sigma_{ox} = 0.223 (\sqrt{m})$  was obtained from the finite element analysis using Equation (4) and a half branch angle of  $\theta_c = 26^\circ$  was obtained using Equation (3). This value is in good agreement with the averaged branch angle of 54 degrees shown in Table 3. Figure 7 shows two frames out of 16-frame dynamic photoelastic record of a branched cracks in a WL-RDCB specimen of 9.5 mm thick, Homalite-100 plate. Experimental details of this series of tests can be found in Reference [28]. Figure 8 shows the dynamic fracture parameters  $K_I$ , and  $\sigma_{ox}$  obtained from the dynamic photoelastic pattern of the three branched cracks shown in Figure 7.  $K_{II}$  which oscillated between  $\pm 0.3 \text{ MPa}\sqrt{m}$  was not plotted in order to avoid cluttering of Figure 7. The decreasing stress intensity factor as well as the fluctuations in  $\sigma_{ox}$  (and  $K_{II}$ ) along the post branching curved cracks are noted. Crack No. 2 arrested at  $K_I = 0.4 \text{ MPa}\sqrt{m}$ . This arrest stress intensity factor is close to arrest stress intensity factor for Homalite-100 determined by Dally [29].

## DISCUSSIONS

Table 1 shows that at the onset of branching, the instantaneous dynamic stress intensity factor reached an average maximum of  $2.04 \text{ MPa}\sqrt{\text{m}}$  irrespective of specimen thickness and loading condition and the initial crack geometry. This branching stress intensity factor,  $K_{Ib}$ , is approximately 4.85 times the fracture toughness and is in agreement with that of Dally [29]. Figures 2 and 3 show that while the  $K_I$  hovers about  $K_{Ib}$ , crack branching will not occur prior to the precipitous drop in  $r_0$ . At the onset of branching, the characteristic  $r_0$  value reaches its average minimum,  $r_c = 1.3 \text{ mm}$  for this material. These results show that  $K_{Ib}$  is a necessary condition for crack branching. The sufficiency condition involves the characteristic distance  $r_0$ , which is a function of the crack velocity,  $K_I$  and  $\sigma_{ox}$ . The ratio of  $K_I$  values prior to and after crack branching is an average of 2.2. Although this value is consistent with the postulate that crack branching occurs to dissipate fracture energy along two propagating cracks, it is higher than the expected  $\sqrt{2}$  value.

It is also interesting to note that  $K_{II} = 0$  prior to crack branching increases a small amount immediately after crack branching consistent with the postulated directional stability model [23]. Irrespective of the crack geometry and specimen thickness, crack branched when it reached  $K_I = K_{Ib}$  and  $r_0 = r_c$ , regardless of crack traveling length.

Of a total of 31 dynamic fracture tests involving WL-RDCB, 14 cracks curved and 6 branched at initiation. These results imply that crack branching in WL-RDCB specimens is observed only in few cases and is attributed to the fact that the crack propagates in a decreasing  $K_I$  field, a situation which does not promote crack branching beyond the initiation of crack extension.

The crack branching angles of Kobayashi [8], Kalthoff [21] and Christie [22] all converged to about 25-28 degrees. This agreement is not surprising since the loading conditions and the specimen geometries are quite similar in all three cases and resulted in negative  $\sigma_{ox}$  value which reduces the fracture angle.

#### CONCLUSIONS

1. A necessary and sufficient condition for dynamic crack branching is a crack branching stress intensity factor,  $K_{Ib}$ , accompanied by minimum characteristic distance  $r_0 = r_c$ .
2. The crack instability model based on the above successfully predicted crack branching angles in Homalite-100 SEN and WL-RDCB specimens.

#### ACKNOWLEDGEMENT

The work reported here was obtained under ONR Contract No. 0014-76-C-0000 NR 064-478. The authors wish to acknowledge the support and encouragement of Dr. Y. Rajapakse, ONR during the course of this investigation.

Table 1

## SUMMARY OF EXPERIMENTAL CRACK BRANCHING DATA AT THE ONSET OF BRANCHING IN

## A SINGLE EDGED NOTCHED SPECIMEN UNDER FIXED GRIP LOADING

Test No.	Plate Thickness h	Initial Crack Length $a_0$	Crack Length Branching $a_b$	c/c <sub>1</sub>	K <sub>Ib</sub>	$\sigma_{ox}$	At Branching		Meas. Branch Angle $\theta_c$	Calc. Branch. Angle $\theta_c$
							r <sub>c</sub>	K <sub>Ib</sub> /K <sub>IC</sub>		
	mm	mm	mm		MPa $\sqrt{m}$	MPa	mm		$\theta_c$	
B8	3.18	5.6	66.0	0.160	2.08	6.93	1.2	4.95	23°	26
B9	3.18	4.3	177.0	0.160	2.03	5.55	1.3	4.83	30°	24
W082270*	3.58	5.8	139.7	0.160	2.03	6.75	1.4	4.83	26°	26
B7**	9.53	5.1	52.6	0.160	2.00	6.80	1.4	4.76	30°	28
B5	9.53	13.5	19.1	0.16	2.08	7.08	1.2	4.95	30°	28
B6	9.53	13.5	28.7	<u>0.16</u>	<u>2.09</u>	<u>7.60</u>	1.3	<u>4.98</u>	<u>28°</u>	<u>32</u>
Average				0.16	2.04	6.70	1.3	4.85	27.8	27.3

\* Second Branching

\*\* Crack Blunted

Table 2  
 $K_{II}$  and  $\sigma_{ox}$  of Arrested Branch  
 Cracks in Figure 4

(a) Inner Branch Crack

	14th Frame	15th Frame
$K_{II}$	0.4 MPa $\sqrt{m}$	0.44 MPa $\sqrt{m}$
$\sigma_{ox}$	0.32 MPa	-0.04 MPa

(b) Outer Branch Crack

	15th Frame	16th Frame
$K_{II}$	0.44 MPa $\sqrt{m}$	0.41 MPa $\sqrt{m}$
$\sigma_{ox}$	0.08 MPa	0.18 MPa

Table 3

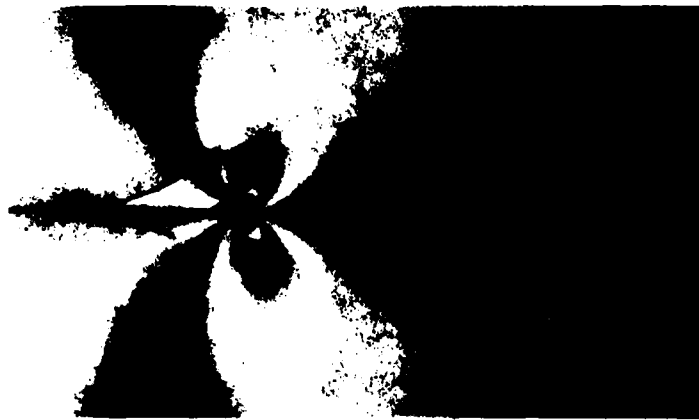
SUMMARY OF CRACK BRANCHING ANGLE DISTRIBUTION IN A WEDGE LOADED RECTANGULAR  
DOUBLE CANTILEVER BEAM SPECIMEN

Test No.	Specimen Thickness	Dia. of Blunt Notch	Measured Branch Angle	Calculated 1st Branch Angle
	$h$ mm	$\rho$ mm	$\theta_c$ 1st Branching	$\theta_c$
L68-120573	9.5	2.2	52	52
L108-052473	9.5	2.2	52	52
L148	9.5	5.0	55	52
L198-013074	9.5	4.0	54	52
L278-022474	9.5	2.4	54	52
		Average	53.4	52

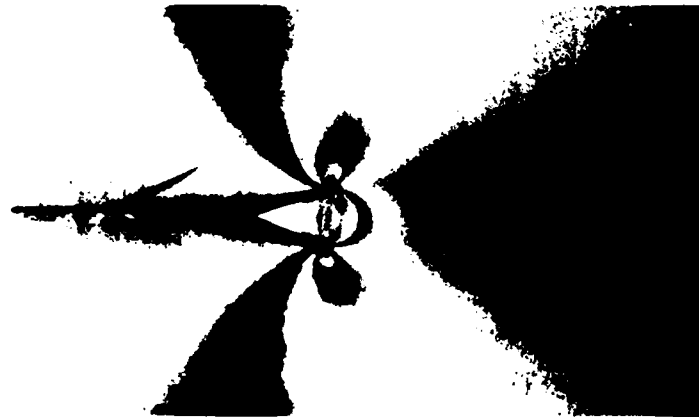
## References

1. Yoffe, E. H., "The Moving Griffith Crack", Phil. Mg., Vol. 42, 1951, pp. 739-750.
2. Achenbach, J. D., "Elasto Dynamic Stress Intensity Factors for a Bifurcated Crack", Prospects of Fracture Mechanics, edited by Sih et al., Noordhoff Int., 1974, pp. 319-336.
3. Achenbach, J. D., "Kinking of a Crack Under Dynamic Loading Conditions", J. Elasticity, Vol. , No. 9, 1979, pp. 113-129.
4. Anthony, S. R., and Congleton, J., "Crack Branching in Metals", Met. Sci., No. 2, 1968, pp. 158-160.
5. Congleton, J., "Practical Application of Crack Branching Measurements", Dynamic Crack Propagation, edited by G. C. Sih, Noordhoff Publ., 1973, pp. 427-438.
6. Irwin, G. R., "Comments on Dynamic Fracturing", ASTM STP 627, 1977, pp. 7-18.
7. Rossmanith, H. P., "Crack Branching in Brittle Materials, Part I", University of Maryland, Photomechanics Laboratory Report, 1977-1980.
8. Kobayashi, A. S., Wade, B. G., Bradley, W. B., and Chiu, S. T., "Crack Branching in Fracturing Homalite-100 Plates", Eng. Fract. Mech., Vol. 6, No. 1, 1974, pp. 81-92.
9. Irwin, G. R., Dally, J. W., Kobayashi, T., Fourney, W. L., Etheridge, M. J. and Rossmanith, H. P., "On the Determination of the a-K Relationships for Birefringent Polymers", Exp. Mech., Vol. 19, No. 4, 1979, pp. 121-128.
10. Kobayashi, A. S., and Ramulu, M., "Dynamic Stress Intensity Factors for Unsymmetric Dynamic Isochromatics", Exp. Mech., Vol. 21, No. 1, 1981, pp. 41-48.
11. Craggs, J. W., "On the Propagation of a Crack in an Elastic Brittle Material", J. Metals Phy. Solids, Vol. 8, 1960, pp. 66-75.
12. Döll, W., "Investigation of a Crack Branching Energy", Int. J. Fract., Vol. 11, 1975, pp. 184-186.
13. Hahn, G. T., Hoagland, R. G., and Rosenfield, A. R., "Crack Branching in A 533B Steel", Fracture 1977, Vol. 2, University of Waterloo Press, 1977, pp. 1333-1338.
14. Kobayashi, T., and Dally, J. W., "The Relation Between Crack Velocity and Stress Intensity Factor in Birefringent Polymers", ASTM STP 627, 1977, pp. 257-273.

15. Kerkhoff, F., "Wave Fractographic Investigation of Brittle Fracture Dynamics", Dynamic Crack Propagation, ed. by G. C. Sih, Noordhoff Int. Publ., Leyden, 1973, pp. 3-35.
16. Schardin, H., "Velocity Effects in Fracture", Fracture, ed. by B. L. Avorbach et al., John Wiley, 1959, pp. 297-330.
17. Acloque, P., "High Speed Cinematographic Study of the Fracture Process in Toughened Glass", Silicate Industrials, Vol. 28, 1963, p. 323.
18. Clark, A.B.J., and Irwin, G. R., "Crack Propagation Behavior", Exp. Mech., Vol. 6, 1966, pp. 321-330.
19. Sih, G. C., "Dynamic Crack Problems: Strain Energy Density Fracture Theory", Elastodynamic Crack Problems, Vol. 4, edited by G. C. Sih, Noordhoff Int. Publishing, Leyden, 1977, pp. 17-37.
20. Kitagawa, H., Yuuki, R., and Ohira, T., "Crack Morphological Aspects in Fracture Mechanics," Eng. Fract. Mech., Vol. 7, 1975, pp. 515-529.
21. Kalthoff, J. F., "On the Propagation of Bifurcated Cracks", Dynamic Crack Propagation, edited by G. C. Sih, Noordhoff Int. Publ., 1973, pp. 449-458.
22. Christie, D. G., "An Investigation of Cracks and Stress Waves in Glass and Plastics by High Speed Photography", Trans. Inc. Glass Tech., Vol. 36, 1952, pp. 74-89.
23. Ramulu, M. and Kobayashi, A. S., "Dynamic Crack Curving - A Photoelastic Evaluation", a paper submitted to Experimental Mechanics.
24. Freund, L. B., "Dynamic Crack Propagation", Mechanics of Fracture, Vol. 19, edited by F. Erdogan, ASME, 1976, pp. 105-134.
25. Streit, R., and Finnie, I., "An Experimental Investigation of Crack Path Directional Stability", Expt. Mech., Vol. 20, No. 1, 1980, pp. 17-23.
26. Bradley, W. B., "A Photoelastic Investigation of Dynamic Brittle Fracture", Ph.D. Dissertation, University of Washington, 1969.
27. Nakasa, K., and Takei, H., "Crack Branching in Delayed Failure", Engr. Fract. Mech., Vol. 11, 1979, pp. 739-751.
28. Lee, M. H., "Dynamic Photoelastic Analysis of a Compression Double Cantilever Beam Specimen", M. Sc. Thesis, University of Washington, 1975.
29. Dally, J. W., "Dynamic Photoelastic Studies of Fracture," Expt. Mech., Vol. 19, No. 10, 1979, pp. 349-367.



FOURTH FRAME  
102  $\mu$  Seconds



FIFTH FRAME  
134  $\mu$  Seconds



SEVENTH FRAME  
212  $\mu$  Seconds

FIGURE 1. TYPICAL CRACK BRANCHING DYNAMIC PHOTOELASTIC PATTERNS  
HOMALITE 100 SINGLE EDGE NOTCHED SPECIMEN (FIXED GRIP  
LOADING) SPECIMEN NO. B8

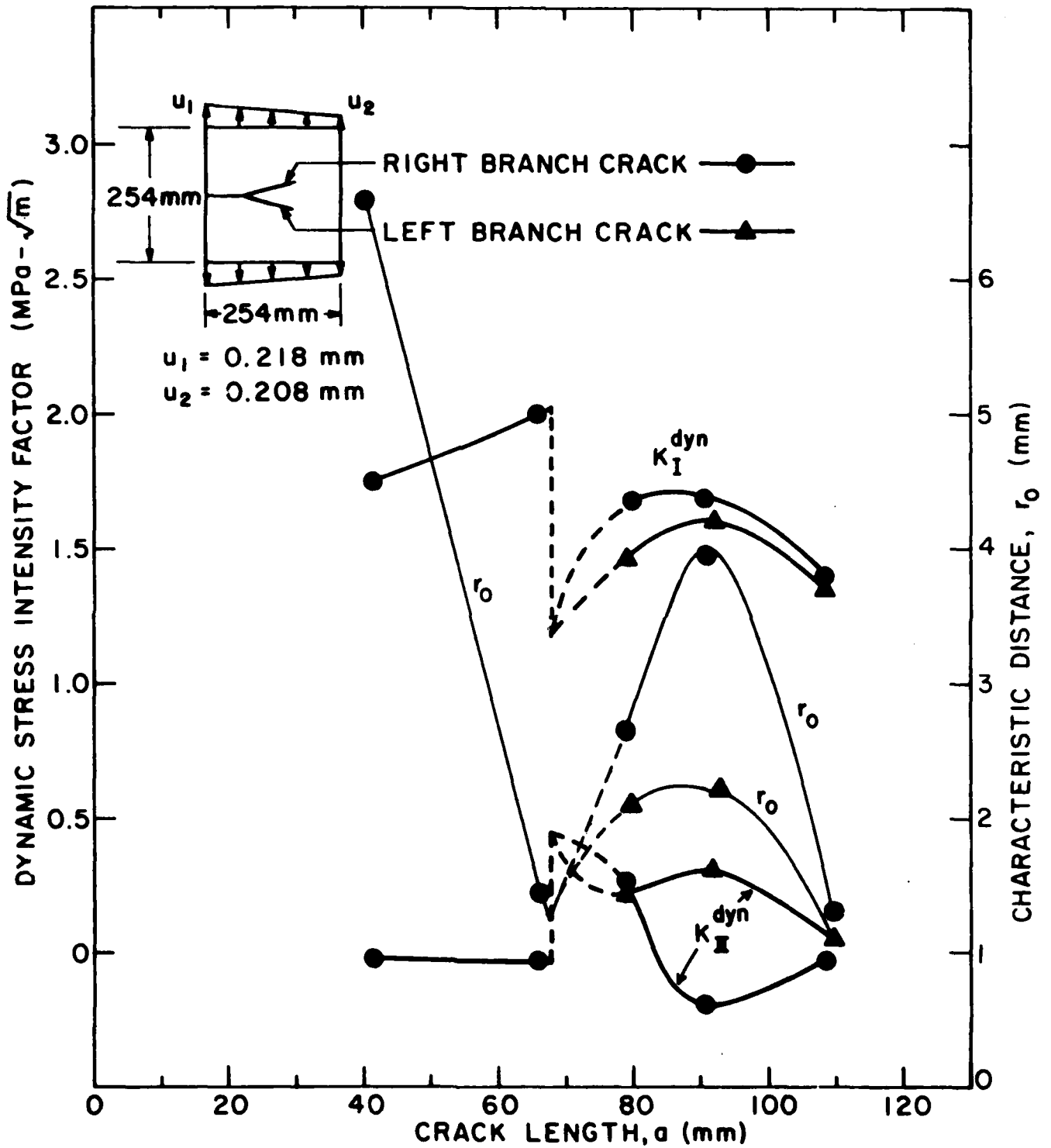


FIGURE 2. DYNAMIC STRESS INTENSITY FACTORS AND  $r_0$  OF BRANCHED CRACKS. SPECIMEN NO. BB.

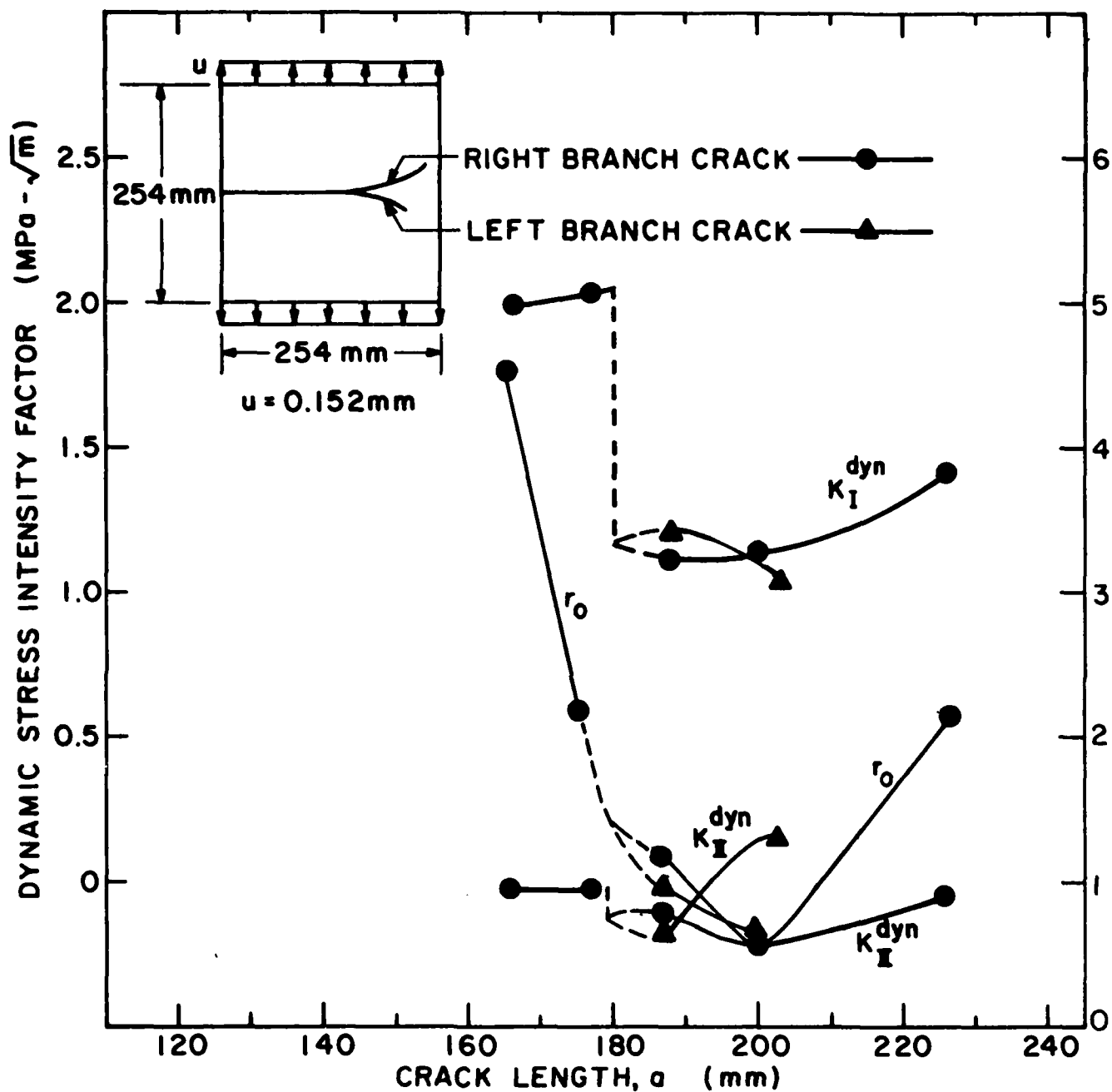


FIGURE 3. DYNAMIC STRESS INTENSITY FACTORS AND  $r_0$  OF BRANCHED CRACKS. SPECIMEN NO. B9.



FOURTEENTH FRAME

448  $\mu$  Seconds



FIFTEENTH FRAME

482  $\mu$  Seconds

(a) INNER BRANCH CRACK



FIFTEENTH FRAME

482  $\mu$  Seconds



SIXTEENTH FRAME

531  $\mu$  Seconds

(b) OUTER BRANCH CRACK

FIGURE 4. TYPICAL MODE II DYNAMIC  
ISOCHROMATIC PATTERNS OF  
ARRESTING BRANCHED CRACKS.  
SPECIMEN NO. B5

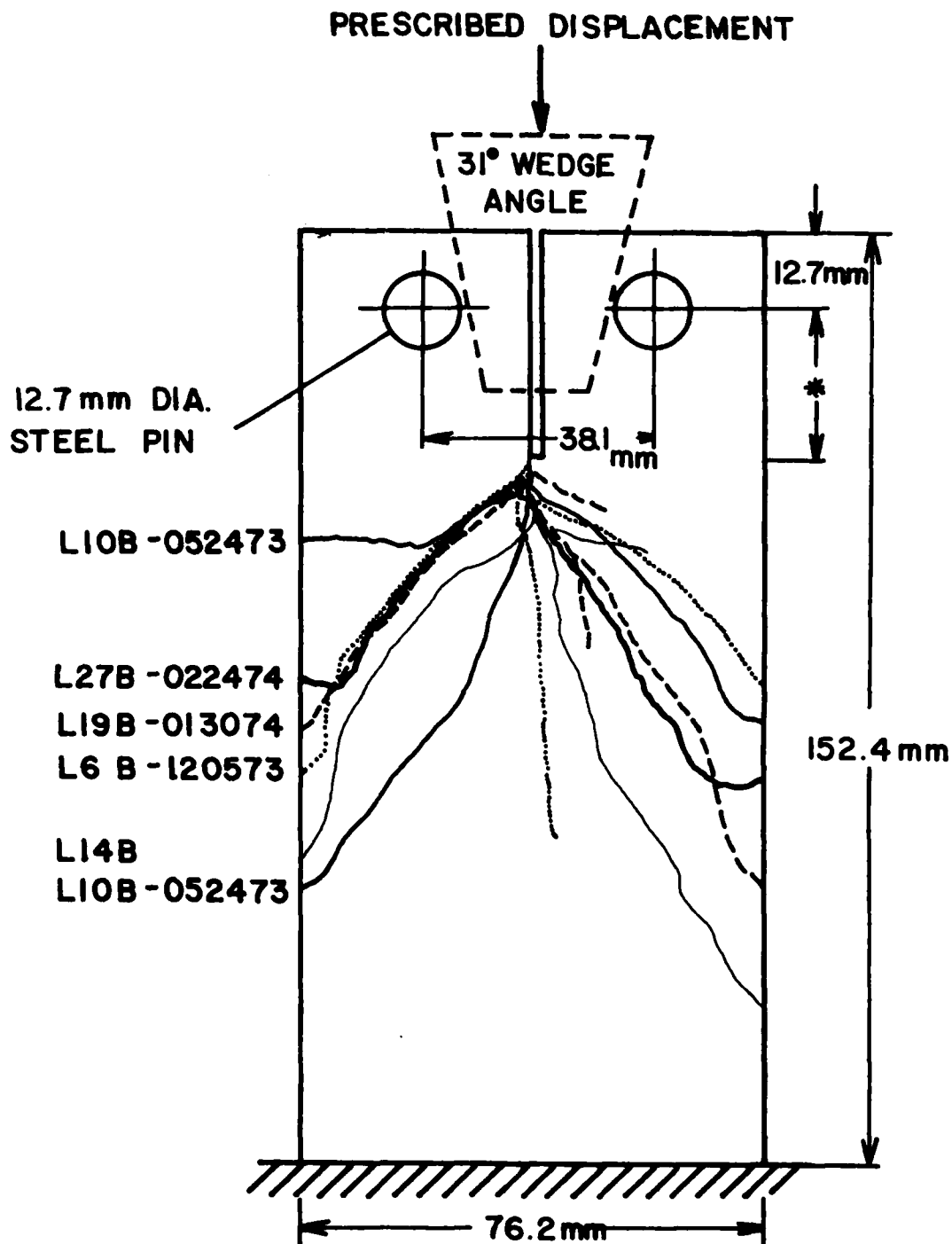


FIFTEENTH FRAME  
482  $\mu$  Seconds



SIXTEENTH FRAME  
531  $\mu$  Seconds

FIGURE 5. DYNAMIC ISOCHROMATIC PATTERNS  
BEFORE AND AFTER CRACK KINKING.  
SPECIMEN NO. B5



\* INITIAL CRACK LENGTH  
NOMINAL THICKNESS 9.5mm

FIGURE 6. BRANCHED CRACK PATHS IN WEDGE LOADED RECTANGULAR DOUBLE CANTILEVER BEAM SPECIMEN (WL- RDCB).



THIRD FRAME, 66  $\mu$  SECONDS



FOURTH FRAME, 84  $\mu$  SECONDS

FIGURE 7. TYPICAL PHOTOELASTIC PATTERNS OF BRANCHED CRACKS  
IN A WEDGE LOADED RECTANGULAR DOUBLE CANTILEVER  
BEAM (WL-RDCB). HOMALITE-100, SPECIMEN NO. L6B-120573.

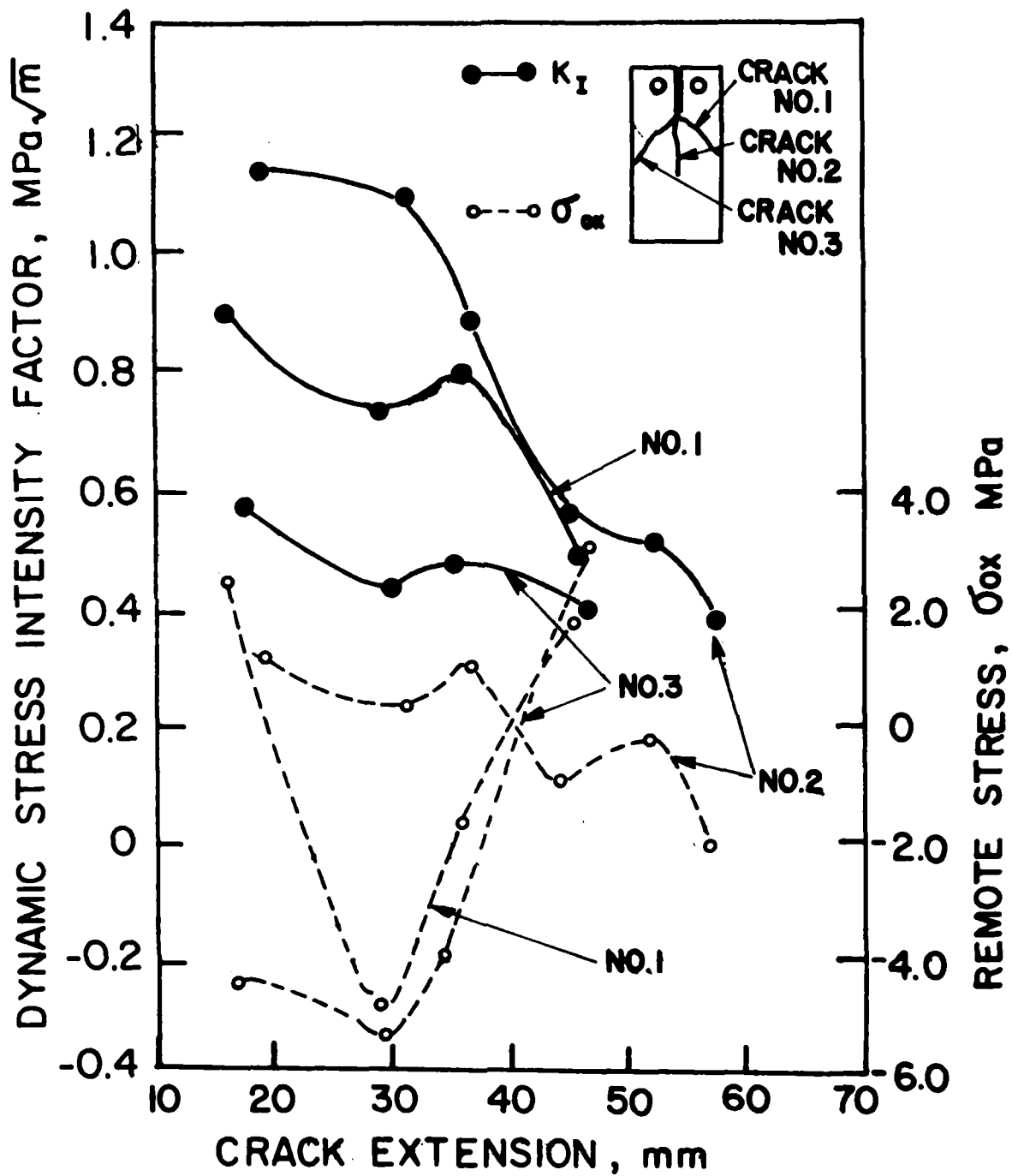


FIGURE 8 . MODE I AND II DYNAMITE STRESS INTENSITY FACTOR OF BRANCHED CRACKS SHOWN IN FIGURE 7 .

474:MP:716:1ab  
78u474-619

Universities (Con't.)

Professor J. Kleener  
Polytechnic Institute of New York  
Department of Mechanical and  
Aerospace Engineering  
333 Jay Street  
Brooklyn, New York 11201

Professor E. A. Schepers  
Texas A&M University  
Department of Civil Engineering  
College Station, Texas 77843

Professor Walter B. Pilkey  
University of Virginia  
Research Laboratories for the  
Engineering Sciences and  
Applied Sciences  
Charlottesville, Virginia 22901

Professor E. D. Elmhurst  
Clarkson College of Technology  
Department of Mechanical Engineering  
Potomac, New York 13676

Dr. Walter E. Rindler  
Texas A&M University  
Aerospace Engineering Department  
College Station, Texas 77843

Dr. Ruesia A. Kama  
University of Arizona  
Department of Aerospace and  
Mechanical Engineering  
Tucson, Arizona 85721

Dr. S. J. Parnes  
Carnegie-Mellon University  
Department of Civil Engineering  
Schenley Park  
Pittsburgh, Pennsylvania 15213

Dr. Donald L. Huston  
Department of Engineering Analysis  
University of Cincinnati  
Cincinnati, Ohio 45221

Universities (Con't.)

Professor G. C. M. Eih  
Lehigh University  
Institute of Fracture and  
Solid Mechanics  
Bethlehem, Pennsylvania 18015

Professor Albert S. Kobayashi  
University of Washington  
Department of Mechanical Engineering  
Seattle, Washington 98105

Professor Daniel Frederick  
Virginia Polytechnic Institute and  
State University  
Department of Engineering Mechanics  
Blacksburg, Virginia 24061

Professor A. C. Eringen  
Princeton University  
Department of Aerospace and  
Mechanical Sciences  
Princeton, New Jersey 08540

Professor F. H. Lee  
Stanford University  
Division of Engineering Mechanics  
Stanford, California 94305

Professor Albert I. King  
Wayne State University  
Biomechanics Research Center  
Detroit, Michigan 48202

Dr. V. B. Hodgson  
Wayne State University  
School of Medicine  
Detroit, Michigan 48202

Don S. A. Riley  
Northwestern University  
Department of Civil Engineering  
Evanston, Illinois 60201

474:MP:716:1ab  
78u474-619

Universities (Con't.)

Professor R. W. Lin  
Syracuse University  
Department of Chemical Engineering  
and Metallurgy  
Syracuse, New York 13210

Professor S. Saday  
Technion R&D Foundation  
Haifa, Israel

Professor Warner Goldsmith  
University of California  
Department of Mechanical Engineering  
Berkeley, California 94720

Professor E. S. Rivlin  
Lehigh University  
Center for the Application  
of Mathematics  
Bethlehem, Pennsylvania 18015

Professor F. A. Cuzzocri  
State University of New York at  
Buffalo  
Division of Interdisciplinary Studies  
Scribner Engineering Building  
Chemistry Hall  
Buffalo, New York 14214

Professor Joseph L. Rose  
Brual University  
Department of Mechanical Engineering  
and Mechanics  
Philadelphia, Pennsylvania 19104

Professor S. K. Donaldson  
University of Maryland  
Aerospace Engineering Department  
College Park, Maryland 20742

Professor Joseph A. Clark  
Catholic University of America  
Department of Mechanical Engineering  
Washington, D.C. 20064

474:MP:716:1ab  
78u474-619

Universities (Con't.)

Dr. Samuel S. Davidoff  
University of California  
School of Engineering  
and Applied Sciences  
Los Angeles, California 90024

Professor Isaac Fried  
Boston University  
Department of Mathematics  
Boston, Massachusetts 02215

Professor E. Krupl  
Rensselaer Polytechnic Institute  
Division of Engineering  
Engineering Mechanics  
Troy, New York 12181

Dr. Jack E. Vinson  
University of Delaware  
Department of Mechanical and Aerospace  
Engineering and the Center for  
Composites Materials  
Rumrort, Delaware 19711

Dr. J. Duffy  
Brown University  
Division of Engineering  
Providence, Rhode Island 02912

Dr. J. L. Smoller  
Carnegie-Mellon University  
Department of Mechanical Engineering  
Pittsburgh, Pennsylvania 15213

Dr. V. E. Varnes  
Ohio State University Research Foundation  
Department of Engineering Mechanics  
Columbus, Ohio 43210

Dr. E. Eshelby  
University of Pennsylvania  
Department of Metallurgy and  
Materials Science  
College of Engineering and  
Applied Sciences  
Philadelphia, Pennsylvania 19104

Universities (Con't.)

Dr. Jackson C. S. Yang  
University of Maryland  
Department of Mechanical Engineering  
College Park, Maryland 20742

Professor T. Y. Chang  
University of Akron  
Department of Civil Engineering  
Akron, Ohio 44325

Professor Charles W. Bert  
University of Oklahoma  
School of Aerospace, Mechanical,  
and Nuclear Engineering  
Norman, Oklahoma 73019

Professor Satya N. Atluri  
Georgia Institute of Technology  
School of Engineering and  
Mechanics  
Atlanta, Georgia 30332

Professor Graham F. Carey  
University of Texas at Austin  
Department of Aerospace Engineering  
and Engineering Mechanics  
Austin, Texas 78712

Dr. S. S. Wang  
University of Illinois  
Department of Theoretical and  
Applied Mechanics  
Urbana, Illinois 61801

Industry and Research Institutes

Dr. Norman Sobbe  
Kaman Airdyne  
Division of Kaman  
Scientific Corporation  
Burlington, Massachusetts 01803

Argonne National Laboratory  
Library Services Department  
9700 South Cass Avenue  
Argonne, Illinois 60460

474:MP:716:1ab  
78u474-619

Industry and Research Institutes (Con't.)

Dr. M. C. Junger  
Cambridge Acoustical Associates  
34 Rindge Avenue Extension  
Cambridge, Massachusetts 02140

Dr. V. Gdina  
General Dynamics Corporation  
Electric Boat Division  
Groton, Connecticut 06340

Dr. J. S. Greenapen  
J. S. Engineering Research Associates  
3831 Manie Drive  
Baltimore, Maryland 21215

Report News Shipbuilding and  
Dry Dock Company  
Library  
Newport News, Virginia 23607

Dr. W. F. Benich  
McDonnell Douglas Corporation  
5301 Balco Avenue  
Huntington Beach, California 92647

Dr. S. M. Abramson  
Southwest Research Institute  
8500 Calobra Road  
San Antonio, Texas 78284

Dr. B. C. DuRant  
Southwest Research Institute  
8500 Calobra Road  
San Antonio, Texas 78284

Dr. H. L. Karno  
Waldinger Associates  
110 East 39th Street  
New York, New York 10021

Dr. T. L. Gault  
Lockheed Missiles and Space Company  
3251 Hammer Street  
Palo Alto, California 94304

Dr. William Caywood  
Applied Physics Laboratory  
Johns Hopkins Road  
Laurel, Maryland 20810

Industry and Research Institutes (Con't.)

Dr. Robert E. Dunham  
Pacifica Technology  
P.O. Box 148  
Del Mar, California 92014

Dr. H. F. Kaminien  
Battelle Columbus Laboratories  
505 King Avenue  
Columbus, Ohio 43201

Dr. A. A. Hochrein  
Dandelion Associates, Inc.  
Springlake Research Road  
15110 Frederick Road  
Woodbine, Maryland 21797

Dr. James W. Jones  
Bussan Service Corporation  
P.O. Box 3413  
Huntington Beach, California 92646

Dr. Robert E. Nichell  
Applied Science and Technology  
1344 North Torrey Pines Court  
Suite 220  
La Jolla, California 92037

Dr. Kevin Thomas  
Westinghouse Electric Corp.  
Advanced Reactors Division  
P. O. Box 158  
Madison, Pennsylvania 15643

Copy available to DTIC does not  
permit fully legible reproduction

**Part 1 - Government  
Administrative and Liaison Activities**

Office of Naval Research  
Department of the Navy  
Arlington, Virginia 22217  
Attn: Code 474 (2)  
Code 471  
Code 200

Director  
Office of Naval Research  
Branch Office  
644 Sumner Street  
Boston, Massachusetts 02210

Director  
Office of Naval Research  
Branch Office  
330 South Clark Street  
Chicago, Illinois 60603

Director  
Office of Naval Research  
Branch Office  
1030 East Grinn Street  
Pasadena, California 91106

Naval Research Laboratory (4)  
Code 2627  
Washington, D.C. 20375

Defense Documentation Center (12)  
Cameron Station  
Alexandria, Virginia 22314

**NAVY**

Undersea Explosions Research Division  
Naval Ship Research and Development  
Center  
Norfolk Naval Shipyard  
Portsmouth, Virginia 23709  
Attn: Mr. E. Palmer, Code 177

**NAVY (Con't.)**

Naval Research Laboratory  
Washington, D.C. 20375  
Attn: Code 8400  
8410  
8430  
8440  
8300  
8390  
8380

David W. Taylor Naval Ship Research  
and Development Center  
Annapolis, Maryland 21402  
Attn: Code 2740  
28  
291

Naval Weapons Center  
China Lake, California 93555  
Attn: Code 4062  
4520

Commanding Officer  
Naval Civil Engineering Laboratory  
Code L31  
Port Hueneme, California 93041

Naval Surface Weapons Center  
White Oak  
Silver Spring, Maryland 20910  
Attn: Code 8-10  
8-402  
8-82

Technical Director  
Naval Ocean Systems Center  
San Diego, California 92152

Supervisor of Shipbuilding  
U.S. Navy  
Norfolk Navy, Virginia 23407

Navy Underwater Sound  
Reference Division  
Naval Research Laboratory  
P.O. Box 8337  
Orlando, Florida 32806

**NAVY (Con't.)**

Chief of Naval Operations  
Department of the Navy  
Washington, D.C. 20330  
Attn: Code 07-096

Strategic Systems Project Office  
Department of the Navy  
Washington, D.C. 20376  
Attn: NSP-100

Naval Air Systems Command  
Department of the Navy  
Washington, D.C. 20361  
Attn: Code 5302 (Aerospace and Structures)  
604 (Technical Library)  
3208 (Structures)

Naval Air Development Center  
Harrisburg, Pennsylvania 17174  
Attn: Aerospace Mechanics  
Code 606

U.S. Naval Academy  
Engineering Department  
Annapolis, Maryland 21402

Naval Facilities Engineering Command  
300 Stovall Street  
Alexandria, Virginia 22332  
Attn: Code 03 (Research and Development)  
048  
045  
14114 (Technical Library)

Naval Sea Systems Command  
Department of the Navy  
Washington, D.C. 20362  
Attn: Code 05H  
312  
322  
323  
05H  
32H

**NAVY (Con't.)**

Commander and Director  
David W. Taylor Naval Ship  
Research and Development Center  
Bethesda, Maryland 20884  
Attn: Code 042  
17  
172  
173  
174  
1800  
1844  
012.2  
1900  
1901  
1943  
1960  
1962

Naval Underwater Systems Center  
Norfolk, Rhode Island 02840  
Attn: Mr. E. Trainor

Naval Surface Weapons Center  
Bagley Laboratory  
Bagley, Virginia 22448  
Attn: Code 004  
020

Technical Director  
Navy Island Naval Shipyard  
Vallejo, California 94592

U.S. Naval Postgraduate School  
Library  
Code 0364  
Monterey, California 93940

Walt Institute of Naval Architecture  
Attn: Librarian  
Crescent Beach Road, Glen Cove  
Long Island, New York 11542

**ARMY**

Commanding Officer (2)  
U.S. Army Research Office  
P.O. Box 12211  
Research Triangle Park, NC 27709  
Attn: Mr. J. J. Murray, CRD-AA-17

474:WP:716:1ab  
78u474-619

**ARMY (Con't.)**

Underwater Arsenal  
Woods Research Center  
Worcester, Massachusetts 02109  
Attn: Director of Research

U.S. Army Materials and Mechanics  
Research Center  
Watertown, Massachusetts 02172  
Attn: Dr. E. Shen, 8422B-7

U.S. Army Missile Research and  
Development Center  
Redstone Scientific Information  
Center  
Chief, Document Section  
Redstone Arsenal, Alabama 35899

Army Research and Development  
Center  
Fort Belvoir, Virginia 22060

**NASA**

National Aeronautics and Space  
Administration  
Structures Research Division  
Langley Research Center  
Langley Station  
Hampton, Virginia 23365

National Aeronautics and Space  
Administration  
Aeronautics Administration for Advanced  
Research and Technology  
Washington, D.C. 20546

**Air Force**

Wright-Patterson Air Force Base  
Dayton, Ohio 45433  
Attn: AFPM (78)  
(78A)  
(78B)  
(78C)  
AFM (78H)

**Air Force (Con't.)**

Chief Applied Mechanics Group  
U.S. Air Force Institute of Technology  
Wright-Patterson Air Force Base  
Dayton, Ohio 45433

Chief, Civil Engineering Branch  
WERC, Research Division  
Air Force Weapons Laboratory  
Kirtland Air Force Base  
Albuquerque, New Mexico 87117

Air Force Office of Scientific Research  
Bolling Air Force Base  
Washington, D.C. 20332  
Attn: Mechanics Division

Department of the Air Force  
Air University Library  
Maxwell Air Force Base  
Montgomery, Alabama 36112

**Other Government Activities**

Commandant  
Chief, Testing and Development Division  
U.S. Coast Guard  
1300 E Street, NW  
Washington, D.C. 20226

Technical Director  
Marine Corps Development  
and Education Command  
Quantico, Virginia 22134

Director Defense Research  
and Engineering  
Technical Library  
Room 3C128  
The Pentagon  
Washington, D.C. 20301

**Other Government Activities (Con't.) PART 2 - Contractors and Other Technical Collaborators**

Dr. H. Gans  
National Science Foundation  
Environmental Research Division  
Washington, D.C. 20530

Library of Congress  
Science and Technology Division  
Washington, D.C. 20540

Director  
Defense Nuclear Agency  
Washington, D.C. 20305  
Attn: SPSS

Mr. Jerome Parish  
Staff Specialist for Materials  
and Structures  
GCHQ/AF, The Pentagon  
Room 3D1009  
Washington, D.C. 20301

Chief, Airframe and Equipment Branch  
PB-120  
Office of Flight Standards  
Federal Aviation Agency  
Washington, D.C. 20533

National Academy of Sciences  
National Research Council  
Ship Hull Research Committee  
2101 Constitution Avenue  
Washington, D.C. 20418  
Attn: Mr. A. E. Lytle

National Science Foundation  
Plastics Mechanics Section  
Division of Engineering  
Washington, D.C. 20530

Precision Arsenal  
Plastics Technical Evaluation Center  
Attn: Technical Information Section  
Bever, New Jersey 07801

Maritime Administration  
Office of Maritime Technology  
14th and Constitution Avenue, NW  
Washington, D.C. 20230

**Universities**

Dr. J. Tinsley Oden  
University of Texas at Austin  
345 Engineering Science Building  
Austin, Texas 78712

Professor Julius Miklowitz  
California Institute of Technology  
Division of Engineering  
and Applied Sciences  
Pasadena, California 91109

Dr. Harold Liebowitz, Dean  
School of Engineering and  
Applied Science  
George Washington University  
Washington, D.C. 20032

Professor Eli Sternberg  
California Institute of Technology  
Division of Engineering and  
Applied Sciences  
Pasadena, California 91109

Professor Paul M. Haghdi  
University of California  
Department of Mechanical Engineering  
Berkeley, California 94720

Professor A. J. Durall  
Oakland University  
School of Engineering  
Rochester, Missouri 48063

Professor F. L. Dilligale  
Columbia University  
Department of Civil Engineering  
New York, New York 10027

Professor Norman Jones  
The University of Liverpool  
Department of Mechanical Engineering  
P. O. Box 147  
Brownlow Hill  
Liverpool L69 3BX  
England

Professor E. J. Shudrath  
Pennsylvania State University  
Applied Research Laboratory  
Department of Physics  
State College, Pennsylvania 16801

COPY 1 to DHC does not  
permit fully legible reproduction

474:WP:716:lab  
78u474-619

Universities (Con't.)

Professor J. Klosser  
Polytechnic Institute of New York  
Department of Mechanical and  
Aerospace Engineering  
333 Jay Street  
Brooklyn, New York 11201

Professor E. A. Schapery  
Texas A&M University  
Department of Civil Engineering  
College Station, Texas 77843

Professor Walter D. Pilkey  
University of Virginia  
Research Laboratories for the  
Engineering Sciences and  
Applied Sciences  
Charlottesville, Virginia 22901

Professor K. D. Willmert  
Clarkson College of Technology  
Department of Mechanical Engineering  
Potomac, New York 13676

Dr. Walter E. Meisler  
Texas A&M University  
Aerospace Engineering Department  
College Station, Texas 77843

Dr. Masao A. Kamel  
University of Arizona  
Department of Aerospace and  
Mechanical Engineering  
Tucson, Arizona 85721

Dr. S. J. Fawcett  
Carnegie-Mellon University  
Department of Civil Engineering  
Schmiley Park  
Pittsburgh, Pennsylvania 15213

Dr. Ronald L. Huston  
Department of Engineering Analysis  
University of Cincinnati  
Cincinnati, Ohio 45221

Universities (Con't.)

Professor G. C. N. Eib  
Lehigh University  
Institute of Structure and  
Solid Mechanics  
Bethlehem, Pennsylvania 18015

Professor Albert S. Kobayashi  
University of Washington  
Department of Mechanical Engineering  
Seattle, Washington 98105

Professor Daniel Frederick  
Virginia Polytechnic Institute and  
State University  
Department of Engineering Mechanics  
Blacksburg, Virginia 24061

Professor A. C. Eringen  
Princeton University  
Department of Aerospace and  
Mechanical Sciences  
Princeton, New Jersey 08540

Professor E. E. Lau  
Stanford University  
Division of Engineering Mechanics  
Stanford, California 94305

Professor Albert I. King  
Wayne State University  
Mechanics Research Center  
Detroit, Michigan 48202

Dr. V. R. Badgson  
Wayne State University  
School of Medicine  
Detroit, Michigan 48202

Dean S. A. Riley  
Northwestern University  
Department of Civil Engineering  
Evanston, Illinois 60201

474:WP:716:lab  
78u474-619

Universities (Con't.)

Professor E. W. Liu  
Syracuse University  
Department of Chemical Engineering  
and Metallurgy  
Syracuse, New York 13210

Professor S. Saday  
Technion R&D Foundation  
Haifa, Israel

Professor Warner Goldsmith  
University of California  
Department of Mechanical Engineering  
Berkeley, California 94720

Professor R. S. Rivlin  
Lehigh University  
Center for the Application  
of Mathematics  
Bethlehem, Pennsylvania 18015

Professor F. A. Connerelli  
State University of New York at  
Buffalo  
Division of Interdisciplinary Studies  
Kart Parker Engineering Building  
Chemistry Road  
Buffalo, New York 14214

Professor Joseph L. Rose  
Branel University  
Department of Mechanical Engineering  
and Mechanics  
Philadelphia, Pennsylvania 19104

Professor S. K. Donaldson  
Aerospace Engineering Department  
College Park, Maryland 20742

Professor Joseph A. Clark  
Catholic University of America  
Department of Mechanical Engineering  
Washington, D.C. 20064

474:WP:716:lab  
78u474-619

Universities (Con't.)

Dr. Samuel S. Nadorff  
University of California  
School of Engineering  
and Applied Science  
Los Angeles, California 90024

Professor Isaac Fried  
Boston University  
Department of Mathematics  
Boston, Massachusetts 02215

Professor E. Krupel  
Rensselaer Polytechnic Institute  
Division of Engineering  
Engineering Mechanics  
Troy, New York 12181

Dr. Jack E. Vinson  
University of Baltimore  
Department of Mechanical and Aerospace  
Engineering and the Center for  
Composite Materials  
Baltimore, Baltimore 19711

Dr. J. Duffy  
Brown University  
Division of Engineering  
Providence, Rhode Island 02912

Dr. J. L. Swadlow  
Carnegie-Mellon University  
Department of Mechanical Engineering  
Pittsburgh, Pennsylvania 15213

Dr. V. E. Carudon  
Ohio State University Research Foundation  
Department of Engineering Mechanics  
Columbus, Ohio 43210

Dr. E. Nishida  
University of Pennsylvania  
Department of Metallurgy and  
Materials Science  
College of Engineering and  
Applied Science  
Philadelphia, Pennsylvania 19104

Universities (Con't.)

Dr. Joshua C. S. Yang  
University of Maryland  
Department of Mechanical Engineering  
College Park, Maryland 20742

Professor T. Y. Chang  
University of Akron  
Department of Civil Engineering  
Akron, Ohio 44325

Professor Charles W. Bart  
University of Oklahoma  
School of Aerospace, Mechanical,  
and Nuclear Engineering  
Norman, Oklahoma 73019

Professor Satya N. Atluri  
Georgia Institute of Technology  
School of Engineering and  
Mechanics  
Atlanta, Georgia 30332

Professor Graham F. Carey  
University of Texas at Austin  
Department of Aerospace Engineering  
and Engineering Mechanics  
Austin, Texas 78712

Dr. S. S. Wang  
University of Illinois  
Department of Theoretical and  
Applied Mechanics  
Urbana, Illinois 61801

Industry and Research Institutes

Dr. Herman Bobbe  
Kaman Avionics  
Division of Kaman  
Sikorsky Corporation  
Burlington, Massachusetts 01803

Argonne National Laboratory  
Library Services Department  
9700 South Cass Avenue  
Argonne, Illinois 60440

474:WP:716:lab  
78u474-619

Industry and Research Institutes (Con't.)

Dr. M. C. Jungner  
Cambridge Aeronautical Associates  
54 Bridge Avenue Extension  
Cambridge, Massachusetts 02140

Dr. V. Gadiou  
General Dynamics Corporation  
Electric Boat Division  
Groton, Connecticut 06340

Dr. J. E. Greenough  
J. E. Engineering Research Associates  
3831 Maple Drive  
Baltimore, Maryland 21215

Navport Navy Shipbuilding and  
Dry Dock Company  
Library  
Navport News, Virginia 23607

Dr. W. P. Smith  
Hobbsell Douglas Corporation  
5301 Balis Avenue  
Huntington Beach, California 92647

Dr. E. H. Abrahamson  
Southwest Research Institute  
8500 Calobra Road  
San Antonio, Texas 78284

Dr. B. C. DeHart  
Southwest Research Institute  
8500 Calobra Road  
San Antonio, Texas 78284

Dr. M. L. Baron  
Vaidinger Associates  
110 East 39th Street  
New York, New York 10022

Dr. T. L. Geers  
Lockheed Missiles and Space Company  
3131 Monover Street  
Folsom, California 94304

Dr. William Caywood  
Applied Physics Laboratory  
Johns Hopkins Road  
Laurel, Maryland 20810

Industry and Research Institutes (Con't.)

Dr. Robert E. Dunham  
Pacific Technology  
P.O. Box 148  
Del Mar, California 92014

Dr. M. P. Kaminian  
Battelle Columbus Laboratories  
505 King Avenue  
Columbus, Ohio 43201

Dr. A. A. Hochrein  
Sandia Associates, Inc.  
Springhouse Research Road  
15110 Frederick Road  
Woodbine, Maryland 21797

Dr. James V. Jones  
Swenson Service Corporation  
P.O. Box 5415  
Huntington Beach, California 92644

Dr. Robert E. Nicholl  
Applied Science and Technology  
1304 South Torrey Pines Court  
Suite 210  
La Jolla, California 92037

Dr. Kevin Thomas  
Westinghouse Electric Corp.  
Advanced Reactors Division  
P. O. Box 158  
Madison, Pennsylvania 15063

Copy available to DTIC does not  
permit fully legible reproduction

Unclassified

SECURITY CLASSIFICATION OF THIS PAGE (When Data Entered)

REPORT DOCUMENTATION PAGE		READ INSTRUCTIONS BEFORE COMPLETING FORM
1. REPORT NUMBER UWA/DME/TR-82/43	2. GOVT ACCESSION NO. AD-A114525	3. RECIPIENT'S CATALOG NUMBER
4. TITLE (and Subtitle) Dynamic Crack Branching - A Photoelastic Evaluation		5. TYPE OF REPORT & PERIOD COVERED Technical Report
7. AUTHOR(s) M. Ramulu, A. S. Kobayashi & B. S.-J. Kang		6. PERFORMING ORG. REPORT NUMBER UWA/DME/TR-82/43
9. PERFORMING ORGANIZATION NAME AND ADDRESS University of Washington Dept. of Mechanical Engineering FU-10 Seattle, WA 98195		8. CONTRACT OR GRANT NUMBER(s) N00014-76-C-0060
11. CONTROLLING OFFICE NAME AND ADDRESS Office of Naval Research Arlington, VA 22217		10. PROGRAM ELEMENT, PROJECT, TASK AREA & WORK UNIT NUMBERS NR 064-478
14. MONITORING AGENCY NAME & ADDRESS (if different from Controlling Office)		12. REPORT DATE May 1982
		13. NUMBER OF PAGES 19
		15. SECURITY CLASS. (of this report) Unclassified
		15a. DECLASSIFICATION/DOWNGRADING SCHEDULE
16. DISTRIBUTION STATEMENT (of this Report) Unlimited Distribution		
17. DISTRIBUTION STATEMENT (of the abstract entered in Block 20, if different from Report)		
18. SUPPLEMENTARY NOTES		
19. KEY WORDS (Continue on reverse side if necessary and identify by block number) Dynamic fracture crack branching, crack curving, dynamic photoelasticity, finite element analysis		
20. ABSTRACT (Continue on reverse side if necessary and identify by block number) A necessary and sufficient condition for crack branching based on a crack branching stress intensity factor, $K_{Ib}$ , accompanied by a minimum characteristic distance of $r_c$ is proposed. This crack branching criterion is evaluated by dynamic photoelastic experiments involving crack branching of six single-edged notch specimens and six wedge-loaded rectangular double cantilever beam speci- mens. Consistent crack branching at $K_{Ib} = 2.04 \text{ MPa}\sqrt{\text{m}}$ and $r_c = 1.3 \text{ mm}$ verified this crack branching criterion. The crack branching angle predicted by		

DD FORM 1473  
1 JAN 73EDITION OF 1 NOV 68 IS OBSOLETE  
S/N 0102-014-6601

Unclassified

SECURITY CLASSIFICATION OF THIS PAGE (When Data Entered)

Unclassified

SECURITY CLASSIFICATION OF THIS PAGE (When Data Entered)

20. (continued)

this crack branching criterion agreed well with those measured in the crack branching experiments.

Unclassified

SECURITY CLASSIFICATION OF THIS PAGE (When Data Entered)

DATE  
ILME  
—8